

Phenomenological Introduction to Neutrino Oscillations

Tanjona R. Rabemananjara*
Universita degli Studi di Milano
Via Celoria 16, Milano 20133, Italy

I. INTRODUCTION

Since the idea of neutrino oscillations has been hypothesized by Potencorvo in 1957 [? ?], important experimental and theoretical developments have emerged from the study of the properties of neutrino. Chief among these findings is the fact that there has to be physics beyond the Standard Model (SM). The theoretical framework of neutrino mixing and masses for explaining neutrino oscillations is now firmly established. To date, the size of the mass-squared difference together with the mixing angles have been measured. However, despite the incredible precision (better than 10%) in measuring the mass-mixing parameters, the picture is not complete yet. The ordering and scale of the neutrino masses is not fully understood yet along with the value of the Dirac-phase δ . Furthermore, flavor oscillations do not probe the nature of the neutrino fields-whether it is Dirac or Majorana.

Various programs worldwide are currently being pursued in order to provide more experimental capabilities to tackle these issues [? ? ? ? ? ? ? ?]. For instance, in order to make a precise measurement of the Dirac phase, an unprecedented amount of neutrino oscillation data will be needed in order to reduce the statistical errors. This could only be achieved with new detectors with larger mass and higher power beams.

This summary project consists of four sections. In Section II, we give a short overview of the experimental probes that led to the discovery of the neutrino oscillations. In Section III, we give the theoretical aspects of the neutrino oscillation probabilities by highlighting the definition of survival probability. Phenomenological results are presented in Section IV. Finally, conclusions and discussion on the remaining opened problems are drawn in Section V.

II. EXPERIMENTAL PROBE OF NEUTRINO OSCILLATION PHENOMENON

Experimental evidence of neutrino oscillations can be studied from various sources: atmospheric neutrinos, nuclear-reactor neutrinos, and neutrino-antineutrino accelerator beams. The atmospheric neutrinos result from the interaction of cosmic rays and the atmosphere and mostly come from the following reactions:

$$\pi^\pm \longrightarrow \mu^\pm + \nu_\mu/\bar{\nu}_\mu, \quad (1)$$

$$\mu^\pm \longrightarrow e^\pm + \nu_e/\bar{\nu}_e + \bar{\nu}_\mu/\nu_\mu. \quad (2)$$

Production of electron-flavor antineutrino $\bar{\nu}_e$ can be accessed from nuclear reactor experiments in which the $\bar{\nu}_e$ are released from the fission of the main isotopes (^{235}U , ^{239}Pu) used in the nuclear reactors. Finally, (anti-)neutrinos can be produced from various collider experiments such as CERN, FNAL, and the Los Alamos Neutron Science Center.

Historically, one of the earliest indication of neutrino oscillations was found in atmospheric neutrino experiments that used radiochemical techniques with the Homestake detector [?]. These experiments measure a flux of electron-flavor neutrinos ν_e , originating from the sun, that was significantly lower than the one expected by the Standard Solar Model (SSM). Because solar ν_e oscillate to different flavors, the detectors which are only sensitive to ν_e detect smaller number of events. This phenomenon has been known as the *solar neutrino problem* and has been confirmed by different neutrino experiments such as GALLEX [? ?], Kamiokande [? ? ?], and Super-Kamiokande [? ?].

The first evidence of neutrino oscillations has been established by studying the atmospheric neutrinos with water [? ?] (Kamiokande and Super-Kamiokande) in 1998. The data exhibit a zenith angle θ dependent deficit of ν_μ which is inconsistent with calculations of neutrino atmospheric fluxes and cannot be explained by the experimental biases and uncertainties. Indeed, if neutrinos do not oscillate, the number of observed atmospheric neutrino is predicted to be uniform. In Fig. 1 we see the number of observed muon-flavor neutrinos as a function of the zenith angle $\cos(\theta)$ from the Super-Kamiokande analyses. This results show that the number of *upward* going muon neutrinos generated from the outer-atmosphere is half of the number of *downward* going muon neutrino.

This observation suggested that neutrinos change flavors as they propagate from their source, (through the medium), to the detectors. Such a mechanism of flavor changes require that the neutrinos have more than one mass state which is not allowed by the SM. For this reason, the neutrino oscillation provided a direct measurement of physics beyond the SM. Hence, the search for understanding of the properties of the neutrinos is considered as one of the most important directions for the search for new physics. To date, more than 40 different experiments is dedicated to the investigation of the problem of neutrino masses and mixing.

III. THEORETICAL FRAMEWORK

Neutrinos interacts with other particles via weak interactions which are described by the charge current (CC)

* tanjona.rabemananjara@mi.infn.it

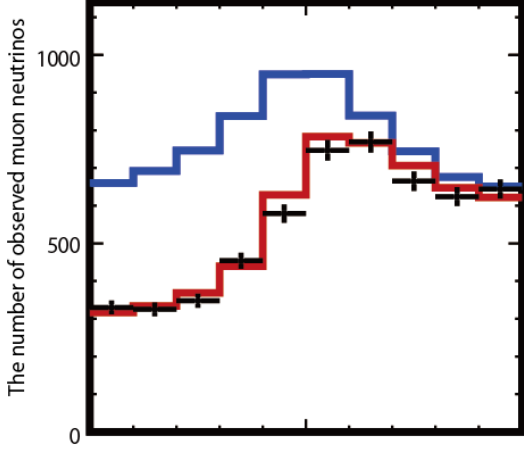


FIG. 1: Observed muon-flavor neutrino from the Super-Kamiokande experiment. The *blue* curve represents the expected number of event without neutrino oscillation, the *red* curve represents the number of events in case of neutrino oscillation, and the *black* crosses represent the observed number of events in the Super-Kamiokande detector.

and neutral current (NC) interaction Lagrangians:

$$\mathcal{L}_{CC} = -\frac{g}{2\sqrt{2}}\mathcal{J}_\rho^{CC}W^\rho + h.c., \quad (3)$$

$$\mathcal{L}_{NC} = -\frac{g}{2\cos(\theta_W)}\mathcal{J}_\rho^{NC}Z^\rho, \quad (4)$$

where g represents the $SU(2)_L$ gauge coupling constant and θ_W the weak angle. Furthermore, the charged and neutral current that are respectively denoted by \mathcal{J}_ρ^{CC} and \mathcal{J}_ρ^{NC} are defined as:

$$\mathcal{J}_\rho^{CC} = 2 \sum_l \bar{\nu}_{lL} \gamma_\rho l_L, \quad (5)$$

$$\mathcal{J}_\rho^{NC} = \sum_l \bar{\nu}_{lL} \gamma_\rho \nu_{lL}, \quad (6)$$

where the charged leptonic field l can be one of the neutrino flavors (e, μ, τ).

If the neutrinos have zero-masses, then the left-handed neutrino field $\nu_{\alpha L}$ with flavor α can be written as a superposition of the left-handed components ν_{iL} of the neutrino field with mass m_i . In an ultra-relativistic scenario, we have:

$$\nu_{\alpha L} = U_{\alpha i} \nu_{iL} \quad (7)$$

where repeated indices are summed over. Henceforth, we use Greek letters to refer to the neutrino masses and Latin letters to refer to the flavours. The neutrino masses i runs from 1 to N where N denotes the number of massive neutrinos. In this project, we are only going to focus in the case $N = 3$.

In Eq. (7), U is a unitary matrix. This implies that a flavor eigenstate $|\nu_\alpha\rangle$ can be written as a superposition

of different mass eigenstates $|\nu_i\rangle$ in the following way:

$$|\nu_{\alpha L}\rangle = U_{\alpha i}^* |\nu_i\rangle, \quad (8)$$

$$|\bar{\nu}_{\alpha L}\rangle = U_{\alpha i} |\bar{\nu}_i\rangle. \quad (9)$$

Assuming that we have three (03) massive neutrinos and that the neutrinos are Dirac particles, the mixing unitary matrix U can be written as:

$$U = \dots, \quad (10)$$

where $c_{ij} = \cos(\theta_{ij})$ and $s_{ij} = \sin(\theta_{ij})$. Here, θ_{ij} denote the mixing angles while δ denotes the Dirac-type CP-phase. Defining $\Delta_{ij} = m_i^2 - m_j^2$ and ordering the masses such that $\Delta_{21}^2 > 0$ and $\Delta_{21}^2 < \Delta_{31}^2$, we have the following constraints:

$$0 \leq \theta_{ij} \leq \frac{\pi}{2} \quad (i \neq j), \quad 0 \leq \delta \leq 2\pi. \quad (11)$$

III.1. Neutrino evolution equation in vacuum and in matter

The evolution equation of a generic neutrino state $|\nu(t)\rangle$ is described by a Shrödinger-like equation:

$$i\partial_t |\nu(t)\rangle = H |\nu(t)\rangle, \quad (12)$$

where H represents the Hamiltonian operator. Expressed in the flavor eigenstate basis $|\nu_\alpha\rangle$, the above equation translates into

$$i\partial_t v^{(f)}(t) = H^{(f)} v^{(f)}(t), \quad (13)$$

where $v^{(f)}(t)$ denotes the vector describing the flavor content of the neutrino state $|\nu(t)\rangle$. Elements of the Hamiltonian matrix $H^{(f)}$ are given by

$$H_{\alpha\beta}^{(f)} = \langle \nu_\alpha | H | \nu_\beta \rangle. \quad (14)$$

In the mass eigenstate basis, the vacuum Hamiltonian $H^{(m)}$ (where m indicates the mass eigenstate representation) is determined in terms of the neutrino masses

$$H_{vac}^{(m)} = \text{diag} \left(\sqrt{\vec{p}^2 + m_1^2}, \sqrt{\vec{p}^2 + m_2^2}, \sqrt{\vec{p}^2 + m_3^2} \right), \\ \approx |\vec{p}| + \frac{1}{2|\vec{p}|} \text{diag} (m_1^2, m_2^2, m_3^2). \quad (15)$$

In the first equality we assumed that the neutrino state $|\nu(t)\rangle$ can be described as a superposition of states with fixed momentum \vec{p} . In the last line, we used the ultra-relativistic approximation $\sqrt{\vec{p}^2 + m_i^2} \sim |\vec{p}| + m_i^2/2|\vec{p}|$. The new Hamiltonian in the flavor eigenstates therefore reads

$$H_{\alpha\beta, vac}^{(f)} = U_{\alpha i} H_{ij, vac}^{(m)} U_{i\beta}^\dagger \quad (16)$$

In the presence of matter, we have to add the vacuum Hamiltonian an effective potential V in the evolution equation

$$i\partial_t |\nu(t)\rangle = (H_{vac} + V) |\nu(t)\rangle, \quad (17)$$

where in the context of SM, the effective potential is a matrix that is diagonal in the flavor basis $V^{(f)} = \text{diag}(V_e, V_\mu, V_\tau)$.

III.2. Survival probability

Assuming that a neutrino is created at a time $t_0 = 0$ at a point $x_0 = 0$, the flavor state $|\nu(t)\rangle$ in the flavor eigenstate basis can be written as

$$\nu^{(f)}(0) = (\langle\nu_e|\nu(0)\rangle, \langle\nu_\mu|\nu(0)\rangle, \langle\nu_\tau|\nu(0)\rangle)^T. \quad (18)$$

After some interval of time t at a given point x , its flavor has evolved according to

$$\nu^{(f)}(x) = S^{(f)}(x)\nu^{(f)}(0), \quad (19)$$

where the evolution operator S is expressed as

$$S^{(f)} = T \left[\exp \left(-i \int_0^x d\tilde{x} H^{(f)}(\tilde{x}) \right) \right]. \quad (20)$$

In the above equation, T represents the time ordering operator. Therefore, the probability to detect a neutrino of flavor ν_β at a distance L from its initial position (where its initial flavor is known) is given by

$$P(\nu_\beta \leftarrow \nu_\alpha) = |S_{\beta\alpha(L)}^{(f)}|^2. \quad (21)$$

This implies that the survival probability $P(\nu_\alpha \leftarrow \nu_\alpha)$ is given by the following

$$P(\nu_\alpha \leftarrow \nu_\alpha) = 1 - P(\nu_\beta \leftarrow \nu_\alpha). \quad (22)$$

The above expression is a consequence of the unitarity of the mixing matrix $\sum_\beta P(\nu_\beta \leftarrow \nu_\alpha) = 1$.

III.3. Vacuum neutrino oscillations

As it was presented in the previous section, in vacuum the neutrino Hamiltonian H is constant. Hence, the evolution operator can be written as

$$S^{(f)} = U S^{(m)} U^\dagger. \quad (23)$$

The evolution operator in the mass eigenstate (denoted by the (m)) is a diagonal matrix that is function of $\phi_i = -m_i^2 x / 2|\vec{p}|$

$$S^{(m)} = \text{diag}(\exp(i\phi_1), \exp(i\phi_2), \exp(i\phi_3)). \quad (24)$$

The probability of observing a neutrino of flavor ν_α to change into a neutrino of flavor ν_β is given by

$$P(\nu_\beta \leftarrow \nu_\alpha) = (U_{\beta i} U_{\alpha i}^* U_{\beta j}^* U_{\alpha j}) \exp(i\phi_{ij}), \quad (25)$$

where in the ultra-relativistic limit $|\vec{p}| \sim E$ and hence $\phi_{ij} = (\Delta_{ij} L) / (2E)$. From this result, we are now equipped with the tools needed to compute the oscillation probabilities. For the case of two neutrino flavor mixing, we only consider one non-vanishing mixing angle θ_{ij} in the evolution operator U described by Eq. (10).

The oscillation probability in Eq. (25) then leads to the following well known result

$$P(\nu_\beta \leftarrow \nu_\alpha) = \sin^2(2\theta_{ij}) \sin^2 \left(\frac{\Delta_{ij}^2 L}{4E} \right). \quad (26)$$

Notice that in the above expression, α has to be different from β ($\alpha \neq \beta$) and depending on the non-vanishing mixing angle, we end up with different flavor changes, i.e.:

$$\theta_{12} \neq 0 \iff P(\nu_\mu \leftarrow \nu_e), \quad (27)$$

$$\theta_{23} \neq 0 \iff P(\nu_\tau \leftarrow \nu_\mu), \quad (28)$$

$$\theta_{13} \neq 0 \iff P(\nu_\tau \leftarrow \nu_e). \quad (29)$$

In the three-neutrino case, by performing the same steps and using further constraint on the masses as introduced previously ($\Delta_{21}^2 \ll |\Delta_{31}^2|$), we have for instance, for $\nu_e \rightarrow \nu_\mu$, the following probability

$$P(\nu_\mu \leftarrow \nu_e) = s_{23}^2 S_{23} \sin^2(2\theta_{13}) + c_{23}^2 S_{12} \sin^2(2\theta_{12}) - 8JS_{12}S_{13}, \quad (30)$$

where $S_{ij} = \sin^2(\Delta_{ij}^2 L / (4E))$ and

$$J = \dots \quad (31)$$

IV. PHENOMENOLOGY OF NEUTRINO OSCILLATION PROBABILITIES

In this section,

IV.1. Numerical insights

From the analytical point of view, computing probabilities of flavor transition involve diagonalizing the Hamiltonian operator. This procedure, however, can be complicated especially when one studies neutrino oscillations in matter. As is often done, careful studies of perturbative methods that lead to some approximations are used in order to compute these probabilities. As described in [], numerical methods can bring new insights into understanding how these probabilities are computed. The resulting methods provide strategies to explore non-standard oscillations where the Hamiltonians do not have generic analytical solutions.

In this project, we follow closely the method described in Ref. [] first introduced by Ohlsson and Snellman in Ref. []. It consists on expanding the Hamiltonian operator that enters in the expression of the evolution operator in terms of $SU(2)$ and $SU(3)$ matrices. The steps for such a calculation can be broken down into the following steps:

- First, the Hamiltonian is expanded in terms of the Pauli matrices in the case of two-neutrino oscillation, and in terms of the Gell-Mann matrices in the case of three-neutrino flavors.

- Compute the coefficients of the expansions in terms of the components of the Hamiltonian.
- The exponent $\exp(iHt)$ is then expanded using the Cayley-Hamilton theorem which states that any analytic function of an $n \times n$ matrix can be written as a polynomial of degree $(n - 1)$ in that matrix.
- Compute the evolution operator in terms of the coefficients in the Hamiltonian series and derive the corresponding probability.

In this report, we only illustrate the case for two-neutrino oscillations. For the three-neutrino case, refer to Ref. [1]. Let us denote the two-neutrino Hamiltonian by H_2 . Its expansion in terms of the Pauli matrices σ^i is given by

$$H_2 = h_0 + h_i \sigma^i \quad (i = 1, 2, 3). \quad (32)$$

The coefficients h_k are fully determined by the components of the Hamiltonian matrix and can be easily computed using the explicit expression of the Pauli matrices.

$$h_0 = \quad (33)$$

The evolution operator U_2 for the two-neutrino oscillations case can therefore be written as

$$U_2 = \exp(-i(h_0 + h_i \sigma^i)L). \quad (34)$$

The first term in the exponent does not affect the probability and therefore can be ignored. Hence, the evolution operator just becomes $U_2 = \exp(-ih_i \sigma^i L)$. Using Euler's formula, the above expression yields

$$U_2 = \cos(|h|L) - \frac{i}{|h|} \sin(|h|L) h_i \sigma^i, \quad (35)$$

where $|h| = \sqrt{|h_1|^2 + |h_2|^2 + |h_3|^2}$. We can now compute the survival probability

$$P(\nu_\alpha \leftarrow \nu_\alpha) = |\nu_\alpha^\dagger U_\alpha \nu_\alpha|^2. \quad (36)$$

Considering $\nu_\alpha = (1, 0)^T$, we can compute the terms that enter in the expression of the probability in Eq. (36)

$$\nu_\alpha^\dagger U_\alpha \nu_\alpha = \cos(|h|L) - i \frac{h_3}{|h|} \sin(|h|L). \quad (37)$$

Putting this expression back into Eq. (36), and with some algebras we can derive the final expression of the survival probability of a neutrino of flavor α ,

$$P(\nu_\alpha \leftarrow \nu_\alpha) = \cos^2(|h|L) + \frac{|h_3|^2}{|h|^2} \sin^2(|h|L). \quad (38)$$

Therefore, the expression of the two-neutrino oscillation probabilities that a neutrino of flavor α is detected with a flavor β is given by the following simple relation:

$$P(\nu_\beta \leftarrow \nu_\alpha) = 1 - P(\nu_\alpha \leftarrow \nu_\alpha). \quad (39)$$

Let us now show that using this approach, we re-derive the two-neutrino oscillation probability given by Eq. (26).

For two-neutrino flavor oscillation, the vacuum Hamiltonian operator is defined as

$$H_2^{vac} = \frac{1}{2E} R_{2,\theta} H_2^{(m)} R_{2,\theta}^\dagger, \quad (40)$$

where $R_{2,\theta}$ represents an Euler rotation with angle θ_{ij} and $H_2^{(m)}$ is given by

$$H_2^{(m)} = \text{diag} \left(\frac{\Delta_{ij}^2}{2}, -\frac{\Delta_{ij}^2}{2} \right). \quad (41)$$

Using the coefficients h_i to compute $|h|$, putting the explicit expression of the coefficients into Eq. (36), and doing some simplification, we arrive at the following expression

$$P(\nu_\beta \leftarrow \nu_\alpha) = \sin^2(2\theta_{ij}) \sin^2 \left(\frac{\Delta_{ij}^2 L}{4E} \right), \quad (42)$$

which is exactly the same as in Eq. (36). The difference being that this approach can be easily implemented numerically to compute oscillations in matter. Going into full details of using this method to compute the three-oscillation probabilities or to study neutrino oscillations in matter is beyond the scope of this project and will be left aside. For complete details and computations, refer to Ref. [1]. The next section, however, will present results beyond the two-neutrino oscillations both in vacuum and in matter.

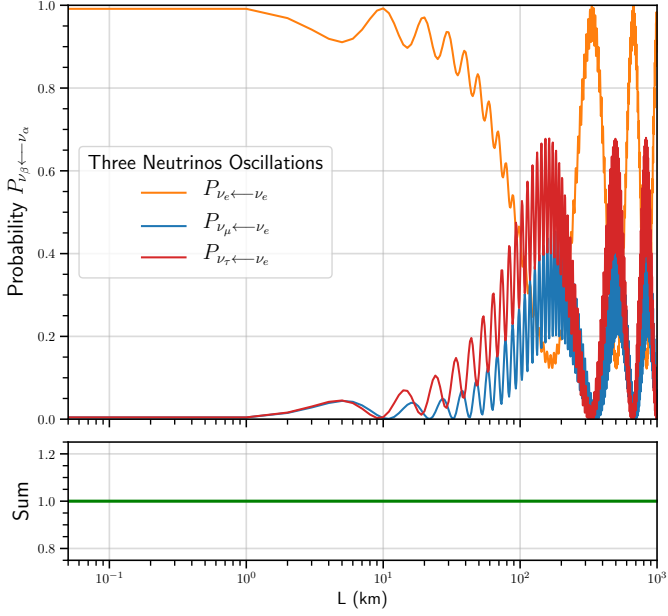
IV.2. Phenomenological results

This section is dedicated to the phenomenological study of the three-neutrino oscillations both in vacuum and in presence of matter with constant density. To compute the oscillation probabilities, the only input parameters that we vary are the energy E and the distance traveled by the neutrino L . The other parameters such as the masses and the mixing angles that enter in the expression of the PMNS mixing matrix are extracted from the NuFit code that fix the parameters to experimental data in order to find the best-fit values. These parameters are summarized in Table I.

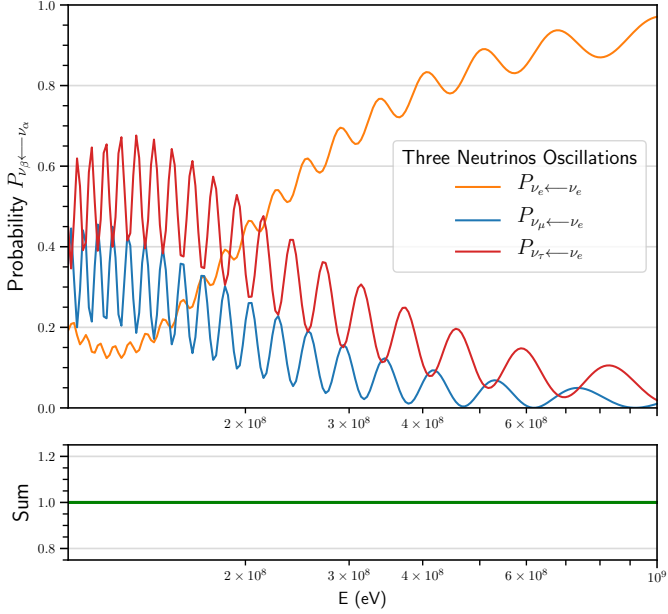
Parameters	Numerical Values
δ_{CP}	217°
$\sin^2 \theta_{12}$	0.310
$\sin^2 \theta_{23}$	0.582
$\sin^2 \theta_{13}$	0.022
Δ_{21}	$7.391 \cdot 10^{-5}$
Δ_{31}	$2.525 \cdot 10^{-3}$

TABLE I: Numerical values of the mass differences Δ_{ij} and mixing angles θ_{ij} extracted from a global fit to oscillation data [20].

The plots shown in this project were produced using python codes [21] which in turn rely on an external



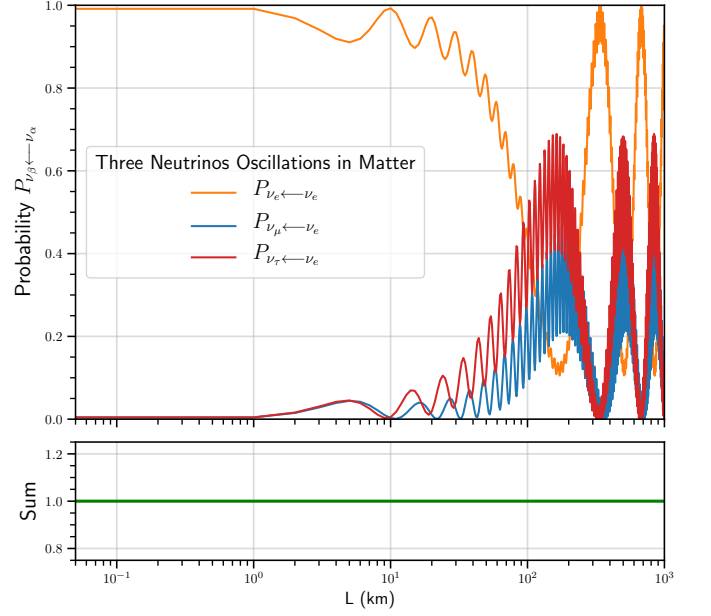
(a) Varying baseline with fixed energy $E = 10^{-2}\text{GeV}$.



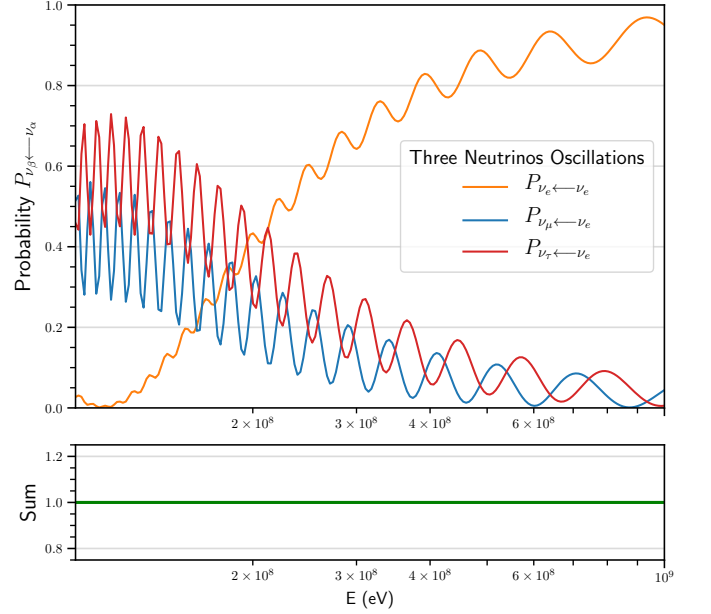
(b) Varying energy with fixed baseline $L = 2 \cdot 10^3\text{km}$.

FIG. 2: Three-neutrino oscillation probabilities in vacuum with varying (a) baseline and (b) varying energy. The top panels show the actual probabilities while the bottom panels shown the sum of the probabilities which exactly sum to one.

python library called NuOsc [1]. In Fig. 2b, we plot the three-neutrino oscillation probabilities as a function of the baseline L and energy E . In particular, we plot the probability that a neutrino with an initial flavor ν_e oscillates between flavors ν_β (with $\beta = e, \mu, \tau$). We can clearly see in the bottom panels that the sum of all probabilities exactly gives one. For small values of L , we see that the probability that the electron-neutrino does not oscillate



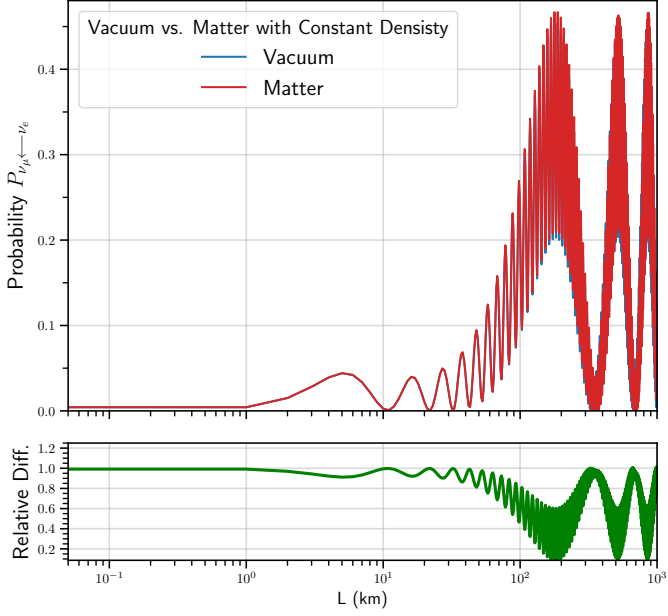
(a) Varying baseline with fixed energy $E = 10^{-2}\text{GeV}$.



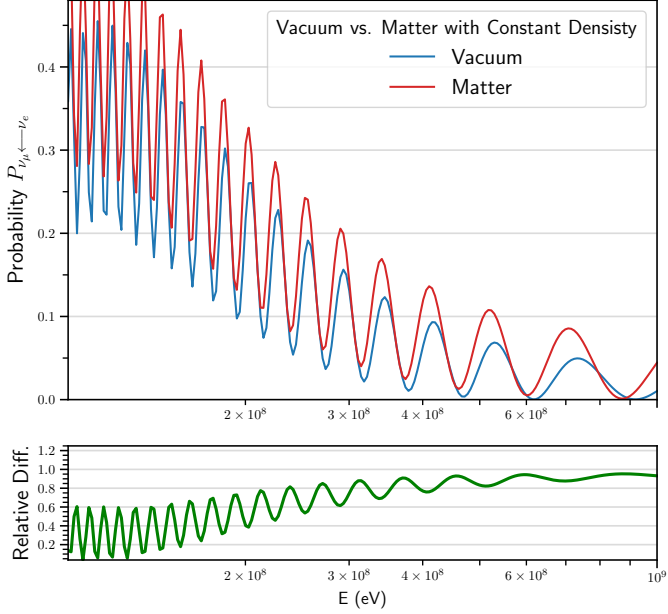
(b) Varying energy with fixed baseline $L = 2 \cdot 10^3\text{km}$.

FIG. 3: Three-neutrino oscillation probabilities in matter with varying (a) baseline and (b) varying energy. The top panels show the actual probabilities while the bottom panels shown the sum of the probabilities which exactly sum to one.

is high. As the neutrino traverses more distances, this probability fluctuates, and in some regions smaller than the probability of the neutrino to have a flavor ν_μ or ν_τ . In the case of probabilities as a function of energy with fixed baseline, we see that instead as the energy increases, the probability that the neutrino keeps the same flavor is higher. In Fig. 3b, we show the three-neutrino oscillation probabilities for a neutrino that propagates in a matter



(a) Varying baseline with fixed energy $E = 10^{-2} \text{ GeV}$.



(b) Varying energy with fixed baseline $L = 2 \cdot 10^3 \text{ km}$.

FIG. 4: Three-neutrino oscillation probabilities in matter with varying (a) baseline and (b) varying energy.

The top panels show the probability $(P_{vac} - P_{mat})/P_{mat}$ both in vacuum and in presence of matter. The bottom panels plot the relative differences.

with constant density $\rho = 3g/cm$. As we can see, the general behavior of the curves look similar to the propagation in vacuum. In order to see the differences, we show in Fig. 4b comparisons between propagation in vacuum and in a matter for $P(\nu_\mu \leftarrow \nu_e)$. The bottom panels show the relative difference $(P_{vac} - P_{mat})/P_{mat}$. We can notice that for small distances (even at small energies), the matter has little effect on the oscillation probability. It is worth mentioning that the propagation in a matter with constant density is the simplest case and does not fully characterize realistic scenarios. A more realistic scenario, for instance, is the study of a neutrino traversing layers of matter, each with constant, but different density as in Ref. [1]. Another well studied phenomena is neutrino oscillation with non-standard interactions. This takes into account the fact that the medium in which the neutrino is propagating in can affect its dynamics Ref. [2].

V. CONCLUSION & OPEN PROBLEMS